Devil's Staircase in Three-Dimensional Coherent Waves Localized on Lissajous Parametric Surfaces

Y. F. Chen,* T. H. Lu, K. W. Su, and K. F. Huang

Department of Electrophysics, National Chiao Tung University, 1001 TA Hsueh Road, Hsinchu 30050, Taiwan
(Received 1 March 2006; published 2 June 2006)

We experimentally demonstrate the significance of the longitudinal-transverse coupling in the mesoscopic regime by using a high-Q laser resonator as an analog experiment. The longitudinal-transverse coupling is found to lead to the three-dimensional (3D) coherent waves that are localized on the parametric surfaces with Lissajous transverse patterns. More strikingly, experimental results reveal that the mode locking of the 3D coherent states forms a nearly complete Devil's staircase with the hierarchical ordering.

PACS numbers: 42.60.Jf, 03.65.Vf, 05.45.−a, 42.55.Xi

The bunch of energy levels in the quantum spectra has been found to lead to the shell structures in nuclei [1], metallic clusters [2], and quantum dots [3]. More intriguingly, the existence of the bunch level has a deep and far-reaching relation with the emergence of classical features in a mesoscopic quantum system [4]. Recent experimental and theoretical studies have verified that the coherent superposition of degenerate or nearly degenerate quantum states can result in mesoscopic quantum wave functions localized on periodic orbits in the classical counterpart of the given system [5]. Furthermore, experimental results [6] indicated that the mode-locking effects lead to the stationary coherent waves associated with periodic orbits to be robust and structurally stable within a finite range of the perturbation or detuning. Devil's staircases, Arnold tongues, and Farey trees are the hallmark of mode locking and have been found to be ubiquitous in physical, chemical, and biological systems [7]. The phenomenon of mode-locked staircases has been extensively studied in Rayleigh-Bénard experiments [8], charge-density-wave systems [9], Josephson-junction arrays [10], reaction-diffusion systems [11], the modulated external-cavity semiconductor laser [12], the driven vortex lattices with periodic pinning [13], the motion of a charge particle in two waves [14], and the bimode CO_2 laser with a saturable absorber [15]. Nevertheless, experiments on the mode-locked staircase in high-order optical coherent waves have never been realized.

In this Letter we originally show that the longitudinal-transverse coupling leads to the formation of three-dimensional (3D) coherent waves localized on *Lissajous* parametric surfaces which are formed by the Lissajous curves with the relative phase varying with the longitudinal direction. A high-Q symmetric laser cavity is experimentally employed to verify the existence and prevalence of 3D coherent waves in the mesoscopic regime. More importantly, the detailed experimental measurements indicate that the formation of plentiful 3D coherent waves constructs a nearly complete devil's staircase in the mesoscopic regime. Since the laser cavity may be used as an excellent analog system for the investigation of quantum

systems [6], the present results will be useful for understanding the mesoscopic wave functions.

The resonance frequency for an optical cavity with two spherical mirrors and the mirror distance L is generally expressed as $f(n, m, l) = \Delta f_L [l + (m + n + 1) \times (\Delta f_T / \Delta f_L)]$, where $\Delta f_L = c/2L$ is the longitudinal mode spacing, Δf_T is the transverse mode spacing, l is the longitudinal mode index, and m and n are the transverse mode indices. For an empty symmetric resonator consisting of two identical spherical mirrors with radius of curvature R, the bare ratio between the transverse and the longitudinal mode spacing is given by $\Omega = \Delta f_T / \Delta f_L = (2/\pi)\tan^{-1}(L/2z_R)$, where $z_R = \sqrt{L(2R - L)}/2$. As a consequence, the bare mode-spacing ratio Ω can be changed in the range between 0 and 1 by varying the cavity length L for a given R. Figure 1 shows a portion of the spectrum $f(l, n, m)$ as a function of the bare mode-spacing ratio Ω for the range of $10 \leq l \leq 30$ and $0 \leq (m + n) \leq 20$. It can be seen that the degeneracies and gaps appear at
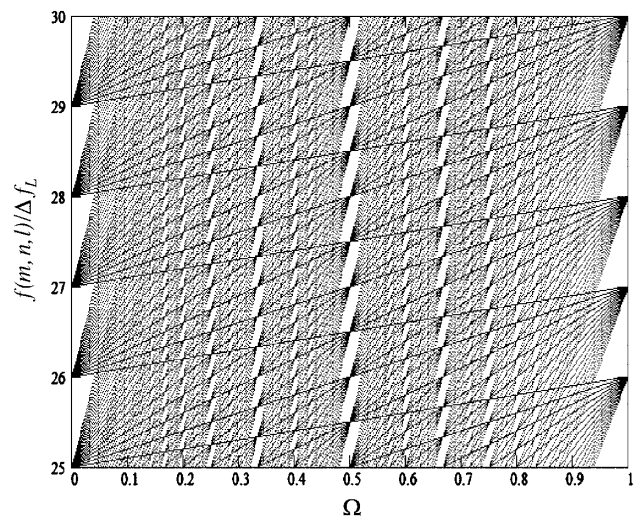
FIG. 1. A portion of the spectrum $f(l, n, m)$ as a function of the bare mode-spacing ratio Ω for the range of $10 \leq l \leq 30$ and $0 \leq (m + n) \leq 20$.

the values of Ω corresponding to the rational numbers P/Q, forming an interesting fractal structure. Degeneracies in the spectra of the quantum systems have been found to play a vital role in the relationship between quantum shell structures and classical periodic orbits, especially in the mesoscopic regime [1–4]. The following

$$\Phi_{m,n,l}^{(\mathrm{HG})}(x, y, z) = \Phi_{m,n}(x, y, z)e^{i(m+n+1)\tan^{-1}(z/z_R)}e^{-i(\pi z/L)[l+(m+n+1)\Omega][(x^2+y^2)/2(z^2+z_R^2)+1]}, \tag{1}$$

where

$$\Phi_{m,n}(x, y, z) = \frac{1}{\sqrt{2^{m+n-1}\pi m! n!}} \frac{1}{w(z)} H_m\left(\frac{\sqrt{2}x}{w(z)}\right) H_n\left(\frac{\sqrt{2}y}{w(z)}\right)$$
$$\times \exp\left[-\frac{x^2 + y^2}{w(z)^2}\right], \tag{2}$$

$w(z) = w_0\sqrt{1 + (z/z_R)^2}$, w_0 is the beam radius at the waist, and z_R is the Rayleigh range. When the mode-spacing ratio Ω is locked to a rational number P/Q, the group of the HG modes $\Phi_{m_0+pk,n_0+qk,l_0+sk}^{(\mathrm{HG})}(x, y, z)$, with $k = 0, 1, 2, 3, \ldots$, can be found to constitute a family of frequency degenerate states, provided that the given integers (p, q, s) obey the equation $s + (p + q)(P/Q) = 0$. For convenience, the integer s is taken to be negative.

analysis will verify that the longitudinal-transverse coupling and the mode-locking effect can lead to the 3D coherent waves to be localized on the parametric surfaces with Lissajous transverse patterns.

The wave functions of the Hermite-Gaussian (HG) modes for a spherical cavity are given by [16]

The equation $s + (p + q)(P/Q) = 0$ indicates that $q + p$ needs to be an integral multiple of Q, i.e., $q + p = KQ$, where $K = 1, 2, 3, \ldots$. It has been verified that the coherent superposition of the mode-locked degenerate states manifestly leads to the wave functions to be associated with the classical periodic orbits in the 2D quantum systems [17]. In the present case, the 3D coherent states constructed by the family of $\Phi_{m_0+pk,n_0+qk,l_0+sk}^{(\mathrm{HG})}(x, y, z)$ can be generally given by $\Psi_{m_0,n_0,l_0}^{p,q,s}(x, y, z; \phi_0) = \sum_{k=0}^{M} e^{ik\phi_0}\Phi_{m_0+pk,n_0+qk,l_0+sk}^{(\mathrm{HG})}(x, y, z)$, where the parameter ϕ_0 is the relative phase between various HG modes at $z = 0$. The relative phase ϕ_0 has been verified to play an important role in the quantum-classical connection [17]. With the expression of Eq. (1), the 3D coherent states can be rewritten as

$$\Psi_{m_0,n_0,l_0}^{p,q,s}(x, y, z; \phi_0) = \Psi_{m_0,n_0}^{p,q}(x, y, z; \phi_0)e^{-i(\pi z/L)[l_0+(m_0+n_0+1)P/Q][(x^2+y^2)/2(z^2+z_R^2)+1]}, \tag{3}$$

where

$$\Psi_{m_0,n_0}^{p,q}(x, y, z; \phi_0) = \sum_{k=0}^{M} e^{ik\phi(z)}\Phi_{m_0+pk,n_0+pk}(x, y, z), \quad (4)$$

and

$$\phi(z) = (q + p)\tan^{-1}(z/z_R) + \phi_0. \tag{5}$$

Equation (3) indicates that the wave pattern of the 3D coherent state $\Psi_{m_0,n_0,l_0}^{p,q,s}(x, y, z; \phi_0)$ is utterly determined by the wave function $\Psi_{m_0,n_0}^{p,q}(x, y, z; \phi_0)$. As seen in Eq. (4), the wave function $\Psi_{m_0,n_0}^{p,q}(x, y, z; \phi_0)$ is a coherent superposition of the modes $\Phi_{m_0+pk,n_0+qk}(x, y, z; \phi_0)$ with the phase factor $\phi(z)$. It is worthwhile to mention that the z dependence of the phase factor $\phi(z)$ arises from the Gouy-phase difference between the HG modes with distinct transverse orders. With the results obtained in the 2D quantum harmonic oscillator [18], the wave function $\Psi_{m_0,n_0}^{p,q}(x, y, z; \phi_0)$ can be manifestly deduced to have the intensity distribution concentrated on the parametric surface:

$$\begin{aligned} x(\vartheta, z) &= \sqrt{m_0 + \frac{M}{2}}w(z)\cos\left[q\vartheta - \frac{\phi(z)}{p}\right]; \\ y(\vartheta, z) &= \sqrt{n_0 + \frac{M}{2}}w(z)\cos(p\vartheta), \end{aligned} \tag{6}$$

where $0 \leq \vartheta \leq 2\pi$ and $-\infty \leq z \leq \infty$. Equation (6) reveals that the parametric surface related to the 3D coherent waves is formed by the Lissajous curves with the relative

phase varying with the position z. In other words, the longitudinal-transverse coupling leads to the 3D coherent states to be localized on the Lissajous parametric surfaces. With $q + p = KQ$ and Eq. (5), the total change of the relative phase of the 3D coherent wave from $z = -\infty$ to $z = \infty$ is given by $\phi(\infty) - \phi(-\infty) = (KQ)\pi$. On the other hand, the total change of the relative phase of the 3D coherent wave from one cavity mirror at $z = -L/2$ to another one at $z = L/2$ is given by $\phi(L/2) - \phi(-L/2) = (KP)\pi$, where the mode-locking condition $\tan^{-1}(L/2z_R) = (P/Q)(\pi/2)$ is used. Figure 2 depicts an example for the Lissajous parametric surface described in Eq. (6) for the range from $z = -L/2$ to $z = L/2$ with $(p, q) = (3, 2)$, $P = 2$, and $\phi_0 = 0$. The tomographic transverse patterns are also plotted in the same figure to display the Lissajous feature of the 3D coherent state. Even though the relationship between the 2D quantum coherent states and the Lissajous curves has been previously developed [17], this is the first time that the 3D coherent states are derived to be related to the Lissajous parametric surfaces.

The wave patterns localized on the classical orbits have been realized in the degenerate laser resonator with the ring-shaped pump profile [19]. However, the index order of the laser modes is not high enough to explore the complete devil's staircase phenomenon in the wave-ray correspondence or quantum-classical correspondence. To generate super-high-order laser modes, here we use the off-axis focused pumping scheme to excite a very high gain crystal in a symmetric cavity with extremely low losses ($<0.5\%$),
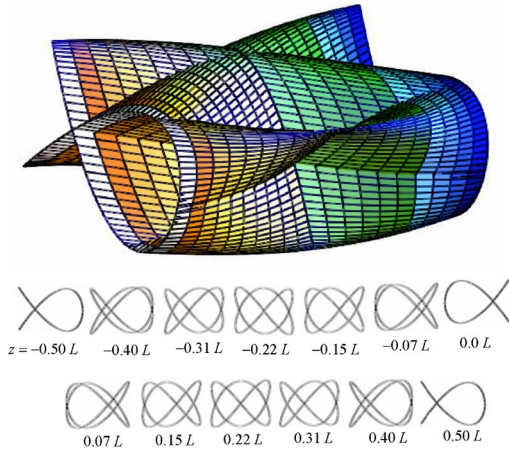
FIG. 2 (color online).   Upper: An example for the Lissajous parametric surface described in Eq. (6) for the range from $z = -L/2$ to $z = L/2$ with $(p, q) = (3, 2)$, $P = 2$, and $\phi_0 = 0$. Bottom: The tomographic transverse patterns along the longitudinal axis.

as depicted in Fig. 3. The laser medium was a a-cut 2.0-at. % Nd^{3+}:YVO_4 crystal with a length of 1 mm. Both sides of the Nd:YVO_4 crystal was coated for antireflection at 1064 nm (reflection <0.1%). The radius of curvature of the cavity mirrors are $R = 10$ mm and their reflectivity is 99.8% at 1064 nm. The pump source was an 809 nm fiber-coupled laser diode with a core diameter of 100 μm, a numerical aperture of 0.16, and a maximum output power of 1 W. A focusing lens with 20 mm focal length and 90% coupling efficiency was used to reimage the pump beam into the laser crystal. The pump radius was estimated to be 25 μm. A microscope objective lens mounted on a translation stage was used to reimage the tomographic transverse patterns inside the cavity onto a CCD camera. To measure the far-field pattern, the output beam was directly projected on a paper screen at a distance of ~50 cm from the rear cavity mirror and the scattered light was captured by a digital camera.

At a pump power of 1 W, the emission powers were generally found to be on the order of 0.5 mW. The low
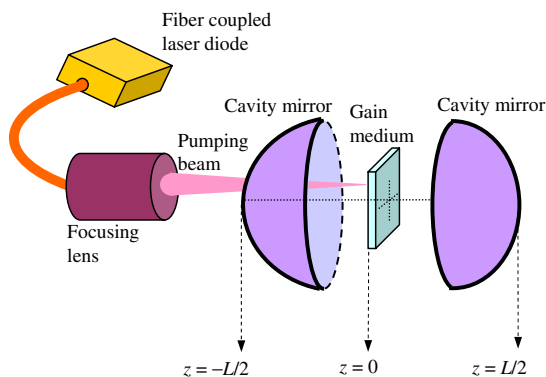
FIG. 3 (color online).   Experimental setup for the generation of 3D coherent waves in a diode-pumped microchip laser with off-axis pumping scheme in a symmetric spherical resonator.

emission powers indicate the cavity Q value to be rather high. The pump positions on the gain medium were controlled to excite the laser modes with the transverse orders n and m in the range of 100 to 500. Experimental results revealed that the far-field transverse patterns were not the familiar HG modes but were almost the coherent waves concentrated on various Lissajous figures for all cavity lengths. Furthermore, the tomographic transverse patterns inside the cavity evidently displayed the revolution of the Lissajous curve along the longitudinal axis to form a Lissajous parametric surface. Figure 4 shows the experimental tomographic transverse patterns observed at $\Omega \approx 0.422$. The experimental tomographic transverse patterns are found to be in good agreement with the feature that the 3D coherent states are well localized on the Lissajous parametric surfaces. Furthermore, the experimental patterns shown in Fig. 4 for $-0.15L \leq z \leq 0.15L$ have a noticeable bright spot that represents the location of the pump beam. It can be seen that the pump intensity has a great overlap with the lasing mode distribution. Since the cavity mode possessing the biggest overlap with the gain region will dominate the laser emission, distinct 3D coherent waves can be precisely generated by manipulating the pump position.

Continuously adjusting the bare mode-spacing ratio Ω, the far-field transverse patterns were found to change from one mode-locked Lissajous wave to another in discrete steps. According to the above-mentioned analysis, the appearance of the Lissajous waves signifies the mode-spacing ratios to be locked to rational numbers P/Q. The analytical representation of the 3D coherent states enables us to identify the mode-locked ratios P/Q precisely from the information of the revolution numbers of the Lissajous wave patterns inside and outside the cavity. Based on thorough experiments, we found that each mode-locked ratio P/Q is composed of numerous 3D coherent waves localized on various Lissajous parametric surfaces with
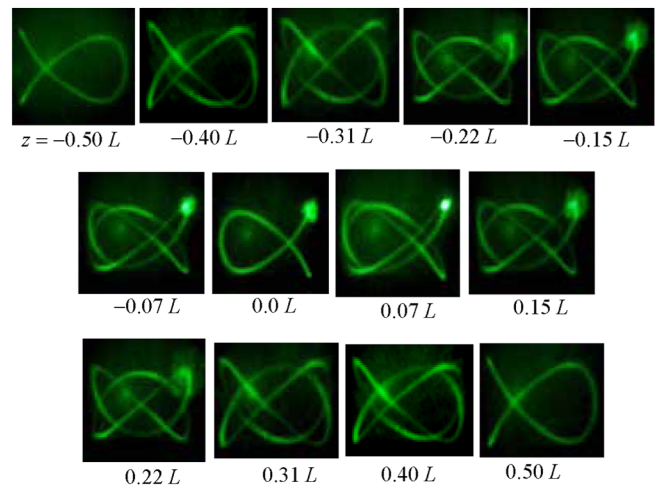
FIG. 4 (color online).   Experimental tomographic transverse patterns inside the cavity observed at $\Omega \approx 0.422$.
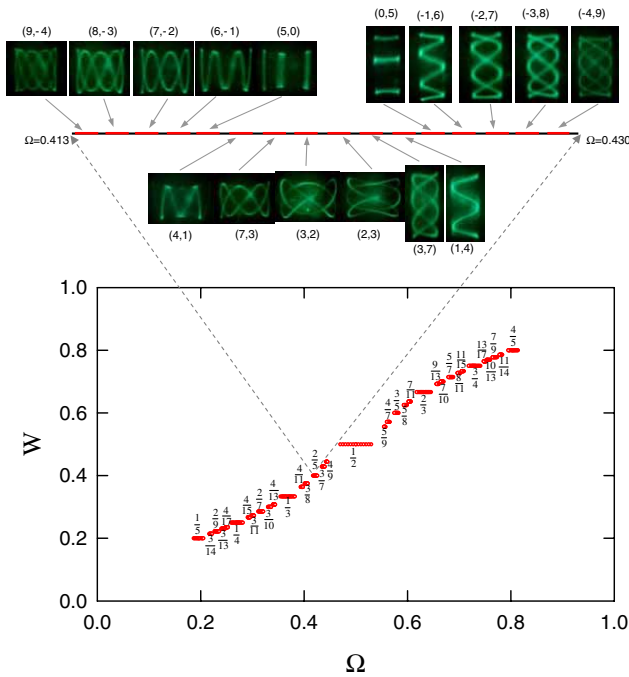
FIG. 5 (color online). Bottom: Experimental mode-locked ratio P/Q as a function of the bare mode-spacing ratio Ω. Upper: Experimental far-field patterns observed in the mode-locked plateau with $P/Q = 2/5$.

indices $q + p$ to be an integral multiple of Q. On the whole, more than 560 different 3D coherent states have been obtained. The locking range of each coherent state was found to be $\Delta\Omega \approx (1.5 \pm 0.2) \times 10^{-3}$ on average. More noticeably, the experimental mode-locked ratios P/Q were found to form a fairly complete devil's staircase, as shown in Fig. 5. Figure 5 also demonstrates the experimental far-field patterns observed in the mode-locked plateau with $P/Q = 2/5$. The absolute values of the indices p and q were first determined from the feature of the Lissajous transverse pattern and their signs were determined from the equation of $q + p = KQ$, where the factor K could be found from the total change of the relative phase of the Lissajous transverse pattern inside the cavity and the indices Q and P were confirmed with the cavity length. It is worthwhile to mention that p and q can have the opposite sign, as long as $q + p$ is an integral multiple of Q. On the other hand, the locking regimes for the coherent states with the indices (p, q) and (q, p) are split due to the anisotropic properties of the gain medium [6]. As the transverse order (m_0, n_0) of the coherent mode is increased, the number of mode-locked plateaus increases, suggesting that all rational steps will be seen in an infinite order system.

In summary, the longitudinal-transverse coupling has been verified to cause the formation of 3D coherent waves with localization on parametric surfaces in the mesoscopic regime. The theoretical analysis reveals that the tomographic transverse patterns of the 3D coherent waves exhibit to be well localized on the Lissajous parametric

surfaces. A high-Q symmetric laser cavity with the off-axis pumping scheme has been utilized to realize the experiment. Experimental results reveal that the mode locking of the 3D coherent states forms a nearly complete devil's staircase with the hierarchical ordering. Our studies may provide some useful insights into the nature of the mesoscopic wave functions.

*To whom correspondence should be address.
Electronic address: yfchen@cc.nctu.edu.tw

[1] A. Bohr and B. R. Mottelson, *Nuclear Structure* (Benjamin, New York, 1975), Vol. 2.
[2] M. Brack, Rev. Mod. Phys. **65**, 677 (1993).
[3] S. M. Reimann and M. Manninen, Rev. Mod. Phys. **74**, 1283 (2002).
[4] R. K. Bhaduri, S. Li, K. Tanaka, and J. C. Waddington, J. Phys. A **27**, L553 (1994); B. L. Johnson and G. Kirczenow, Europhys. Lett. **51**, 367 (2000).
[5] I. V. Zozoulenko and K. F. Berggren, Phys. Rev. B **56**, 6931 (1997); R. Narevich, R. E. Prange, and O. Zaitsev, Phys. Rev. E **62**, 2046 (2000).
[6] K. F. Huang, Y. F. Chen, H. C. Lai, and Y. P. Lan, Phys. Rev. Lett. **89**, 224102 (2002); Y. F. Chen and Y. P. Lan, Phys. Rev. A **66**, 053812 (2002); Y. F. Chen, K. F. Huang, H. C. Lai, and Y. P. Lan, Phys. Rev. E **68**, 026210 (2003).
[7] H. G. Shuster, *Deterministic Chaos* (VCH Verlag, Weinheim, 1988); E. Ott, *Chaos in Dynamic System* (Cambridge University Press, Cambridge, 1993); A. Pikovsky, M. Rosenblum, and J. Kurths, *Synchronization* (Cambridge University Press, Cambridge, 2001).
[8] J. Stavans, F. Heslot, and A. Libchaber, Phys. Rev. Lett. **55**, 596 (1985).
[9] S. E. Brown, G. Mozurkewich, and G. Grüner, Phys. Rev. Lett. **52**, 2277 (1984); A. A. Middleton, O. Biham, P. B. Littlewood, and P. Sibani, Phys. Rev. Lett. **68**, 1586 (1992).
[10] P. Alstrøm and M. T. Levinsen, Phys. Rev. B **31**, 2753 (1985); E. Orignac and T. Giamarchi, Phys. Rev. B **64**, 144515 (2001).
[11] A. L. Lin, M. Bertram, K. Martinez, and H. L. Swinney, Phys. Rev. Lett. **84**, 4240 (2000).
[12] D. Baums, W. Elsässer, and E. O. Göbel, Phys. Rev. Lett. **63**, 155 (1989).
[13] C. Reichhardt and F. Nori, Phys. Rev. Lett. **82**, 414 (1999).
[14] A. Macor, F. Doveil, and Y. Elskens, Phys. Rev. Lett. **95**, 264102 (2005).
[15] D. Hennequin, D. Dangoisse, and P. Glorieux, Phys. Rev. A **42**, 6966 (1990).
[16] A. E. Siegman, *Lasers* (University Science Books, Mill Valley, CA, 1986).
[17] Y. F. Chen, K. F. Huang, and Y. P. Lan, Phys. Rev. E **66**, 046215 (2002); **66**, 066210 (2002); Y. F. Chen and K. F. Huang, Phys. Rev. E **68**, 066207 (2003).
[18] Y. F. Chen and K. F. Huang, J. Phys. A **36**, 7751 (2003).
[19] Y. F. Chen, Y. P. Lan, and K. F. Huang, Phys. Rev. A **68**, 043803 (2003).